# GRAPHIC DELAY EQUALIZER

*Jussi Rämö and Vesa Välimäki*

Acoustics Lab, Department of Signal Processing and Acoustics,
Aalto University, Espoo, Finland
jussi.ramo@aalto.fi

**ABSTRACT**

A graphic delay equalizer based on a high-order nonparametric allpass filter design is proposed. Command points at the centers of octave frequency bands are connected with polynomial interpolation to form a continuous target group-delay curve as function of frequency. The required number of allpass sections depends on the area under the target curve. The group-delay area at low audio frequencies is small due to the linear frequency scale, so only a few allpass sections can be assigned there, which reduces the accuracy. Design accuracy can be improved by adding a constant delay to the target curve, which increases the area. Two use cases are presented: the group-delay equalization of a multi-way loudspeaker and the linearization of the phase response of a regular magnitude-only graphic equalizer. The graphic delay equalizer can be used to enhance the perceptual quality of audio systems or to produce audio effects.

***Index Terms—*** Audio systems, delay systems, equalizers, phase distortion, psychoacoustics.

## 1. INTRODUCTION

The perception of phase in audio signals is one of the eternal questions in acoustics and audio technology. Helmholtz famously stated that the human hearing is sensitive to the relative strengths of spectral components but not to the differences in their phase [1, 2]. However, afterwards it has been learned that phase differences can be perceived although not as accurately as variations in the magnitude spectrum [3, 2, 4, 5]. The perceptually relevant phase equalization of audio systems, such as loudspeakers, remains a research topic and is among the last unsolved questions in high-fidelity audio [6, 7]. This work proposes a new tool, the graphic delay equalizer, for studying and implementing phase differences.

Many studies have reported that the mean group-delay threshold for audibility is around 2 ms at middle frequencies [8, 9, 10, 11, 6]. However, listening conditions, such as headphone playback, and anechoic or reverberant loudspeaker playback, have a significant impact on the results [12]. Furthermore, the majority of the studies used short impulses as test signals to emphasize the audible perception [12, 4, 6]. All in all, the effects of group delay become more difficult to hear with ecologically valid program material in a reverberant room than with headphones. Applications of delay equalization include phase or group-delay modification of audio systems, such as loudspeakers [13, 14, 15, 7], modeling of dispersive acoustic systems, such as piano strings [16] and spring-reverberation devices [17, 18], and spectral delay effects [19, 20].

This paper proposes a novel concept of a graphic delay equalizer, which is based on a high-order allpass (AP) filter. It can modify the group delay of an audio signal with the same ease as a standard graphic equalizer modifies the magnitude spectrum [21, 22]. The target group-delay response can be controlled at the centers of octave or third-octave bands, which are connected with polynomial interpolation to form a continuous target group-delay curve. Unlike in magnitude-only equalization in which a filter of constant order is controlled at each command band [22], the required number of AP sections depends on the area under the target curve. It is shown how the accuracy of approximation can be increased by adding a constant term to the target group delay. The goal is to design a perceptually sufficient imitation of the target group delay, for example so that the error in group delay is less than 2 ms at middle frequencies.

This paper is organized in the following way. Section 2 recapitulates an existing high-order allpass filter design method, which is used here to develop the graphic group-delay equalizer. Section 3 proposes the novel concept of the graphic delay equalizer. Section 4 discusses two use cases for the proposed method, and Section 5 concludes this paper.

## 2. HIGH-ORDER ALLPASS FILTER DESIGN

The underlying AP filter design that is used to implement the graphic delay equalizer is based on a method proposed by Abel and Smith [23]. In general, a second-order AP filter section has the form

$$H(z) = \frac{a_2 + a_1 z^{-1} + z^{-2}}{1 + a_1 z^{-1} + a_2 z^{-2}}, \tag{1}$$

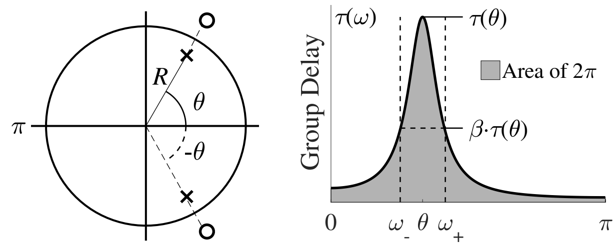


(a) (b)

**Fig. 1**. Second-order allpass filter properties: (a) complex conjugate pole-zero pairs and (b) group delay of the allpass filter in (a). Adapted from [23].

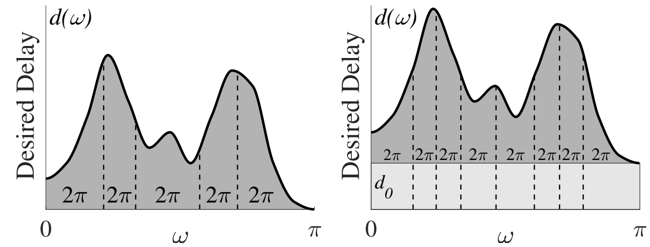


(a) (b)

**Fig. 2**. Automatic segmentation of the user-desired target delay $d(\omega)$ to $2\pi$ sections (a) without additional delay and (b) with an added constant delay $d_0$ in order to increase the accuracy of approximation.

with

$$a_1 = -2R\cos(\theta), \tag{2}$$

$$a_2 = R^2, \tag{3}$$

where $R$ is the radius of complex conjugate poles, and $\pm\theta$ are the angles of the poles [24]. Figure 1(a) shows the poles and zeros of a second-order AP section, when $\theta = 1$ and $R = 0.82$.

The method described by Abel and Smith [23] is based on the founding that a second-order AP filter generates a group-delay function $\tau(\omega)$ with a peak at the pole frequency $\tau(\theta)$ and an area of $2\pi$ regardless of the pole frequency $\theta$ or the pole radius $R$. In other words, the integral of the group-delay function from 0 to $\pi$ is always $2\pi$, as illustrated in Fig. 1(b). Furthermore, it is known that the group delay of a cascaded AP system is the sum of the individual (second-order) AP group delays, which led to the idea of dividing a desired group-delay function $d(\omega)$ into $2\pi$ sections, and assigning a second-order AP filter to each of those $2\pi$ sections [23]. The segmentation is illustrated in Fig. 2(a).

After the target group delay has been divided into $2\pi$ sections, the pole frequency $\theta$ is positioned in the middle of each band

$$\theta = \frac{\omega_+ + \omega_-}{2}, \tag{4}$$

where $\omega_+$ and $\omega_-$ are the calculated band edges containing the $2\pi$ area [23], see Fig. 1(b). The pole radius $R$ is selected so that the group delay at the band edges is a fraction $\beta$ of the maximum group delay peak $\tau(\theta)$, see Fig. 1(b). This leads to a pole radius of

$$R = \eta - (\eta^2 - 1)^{1/2}, \tag{5}$$

where

$$\eta = \frac{1 - \beta\cos(\Delta)}{1 - \beta} \quad \text{with} \quad \Delta = \frac{\omega_+ - \omega_-}{2}. \tag{6}$$

By examining (4)–(6), it can be seen that the AP sections can be implemented by knowing only the band edges $\omega_+$ and $\omega_-$, and the user-defined parameter $\beta$. The parameter $\beta$ controls the sharpness of the individual group-delay functions, thus also controlling the amount of overlap between adjacent group-delay functions within the system. In practice, when $\beta$ is large (close to 1), the system creates smooth group delays, while a small value of $\beta$ results in a more accurate narrow-band design. However, small $\beta$ values can create unwanted ripple, when the target delay curve is smooth [23].

Another way to make the AP system more accurate is to add a constant delay $d_0$ to the system. This creates a larger area under the target delay curve, i.e., more $2\pi$ sections, leading to a larger number of AP filters in the final system than without the extra delay, as illustrated in Fig. 2(b).

## 3. GRAPHIC DELAY EQUALIZER

A graphic equalizer has a set of peak/notch filters with predetermined center frequencies and bandwidths [22]. In other words, the only user-controllable variables are the filter gains, which are implemented using a set of sliders which "plot" the magnitude response of the equalizer. A typical graphic equalizer is implemented using an octave or a third-octave spacing for the command gains. Furthermore, in audio processing, frequencies are often plotted using a logarithmic scale (using Hz) instead of a linear one depicted in Figs. 1 and 2. The logarithmic frequency scale corresponds more closely to how humans perceive sound, see e.g., [25, Ch. 3].

When angular frequencies $\omega$ are converted to Hertz, $2\pi \Rightarrow f_s$, while $\pi \Rightarrow f_s/2$, where $f_s$ denotes the sampling frequency. This means that the $2\pi$ area segments, under the desired delay $d(f)$, become $f_s$-sized area segments, and can be calculated with

$$\int_{f_-}^{f_+} d(f)\,df = f_s, \tag{7}$$

where $f_-$ and $f_+$ correspond to Hz values of $\omega_-$ and $\omega_+$.

Figure 3 illustrates the difference between linear and logarithmic frequency scales, and how it affects the area below the desired delay curve $d(f)$. The vertical dashed lines in

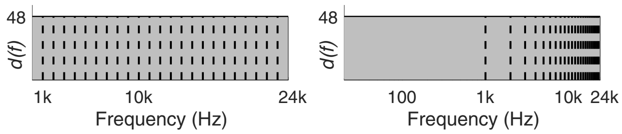


**Fig. 3**. The area below (left) linear frequency scale vs. (right) logarithmic frequency scale, plotted from 20 Hz to 24 kHz.

Fig. 3 divide the area in $f_s$-sized segments, corresponding to $2\pi$ segments in Fig. 2(a). Both figures show the same $f_s$-sized areas, when the desired delay is a constant 48 samples and the sample rate $f_s$ is 48 kHz. The $f_s$-sized segments occur every 1000 Hz, e.g., the first segment is from 0 to 1 kHz. As can be seen in Fig. 3 (left), the $f_s$-sized segments are equally spaced, as expected. However, in Fig. 3 (right), it is illustrated how the first segment already covers approximately half of the total area, when plotted with logarithmic frequency, limiting the accuracy at low frequencies.

### 3.1. Implementation

This section describes the implementation of an octave-band graphic delay equalizer, where the user can control the amount of delay using a set of sliders with center frequencies spaced an octave apart, the value(s) of $\beta$, and the total number of AP sections. After the user has set these parameters, the underlying algorithm will calculate the set of AP filters as follows. First, a target curve $d(f)$ for the desired delay is interpolated from the user-set command delay points using cubic Hermite polynomial interpolation (`pchip` in Matlab).

Second, the area under $d(f)$ is calculated and divided into $f_s$-sized segments, see Fig. 2(a). The required number of AP sections depends on the number of the sections under the target delay curve $d(f)$. Thus, if the user has requested more AP sections than needed to cover the area under $d(f)$, a constant delay $d_0$ is added to $d(f)$ in order to have more $f_s$-sized segments, see Fig. 2(b). This improves the resolution of the equalizer, but increases the total delay.

Third, a second-order AP filter is assigned to each section by calculating $\theta$ and $R$ with (4) and (5), respectively, and substituting those results to (2) and (3) in order to calculate the filter coefficients $a_1$ and $a_2$. Figure 4 shows a design example of an octave-band graphic equalizer, where the user-defined command delays are set to 3.2, 8.4, 5.5, and 6.7 ms at frequencies 1, 2, 4, and 8 kHz, respectively. There is an additional delay $d_0$ of 5.2 ms in order to increase the number of AP sections from 48 (without $d_0$) to 90. The value of $\beta$ is 0.9, in all AP sections. Moreover, the command delay points at 125, 250, 500 Hz, and 16 kHz (gray filled markers) are not in use, i.e., they are turned off. If they were turned on and set to zero, the added constant delay $d_0$ would affect those frequencies as well, and a different result would be obtained, since the area under the target delay curve would have changed.

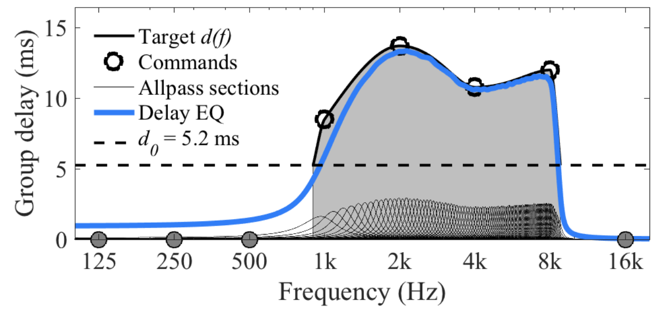


**Fig. 4**. Octave-band graphic delay equalizer (EQ) example: The round markers depict the user set command delays (plus $d_0$), the thin lines are the group delays of AP filters, and the thick (blue) line shows the group-delay approximation.

The user can also fine-tune the delay equalizer by adjusting the values of $\beta$ within the individual AP sections. Typically, this might be helpful with the lowest AP filters, due to the lower integrated area compared to higher frequencies, see Fig. 3. For example, it can be seen in Fig. 4 that the delay equalizer is less accurate at frequencies between 1 and 2 kHz when compared to its accuracy at frequencies above 2 kHz. By tuning the $\beta$ parameter, the user can vary sharpness of the individual group delay peaks of the AP filters. It should be noted that the center frequencies as well as the number of AP filters will be changed, when the user varies the delay gains.

## 4. APPLICATION USE CASES

### 4.1. Delay equalization of a two-way loudspeaker

Figure 5 shows an example of correcting a loudspeaker group delay properties. The loudspeaker group delay shown in Fig. 5(a) is obtained from a two-way loudspeaker model, which has a high-order crossover filter at 900 Hz and a driver-enclosure roll-off at 50 Hz with an additional Helmholtz resonance at 35 Hz [7]. This creates a delay bump of about 3 ms around the crossover frequency, while towards high frequencies the delay goes down towards zero. Since the delay at 900 Hz is more than 2 ms larger than at high frequencies, it can be audible [6]. Furthermore, the highpass behaviour of the speaker at low frequencies creates a large amount of delay, as also seen in Fig. 5(a), but it may be inaudible [6].

The dash-dotted line in Fig. 5(a) shows the group delay of the loudspeaker while the thin (blue) line is the group-delay response of the graphic delay equalizer. The thick line shows the corrected loudspeaker group delay, i.e., the combination of the original group delay and the user-set delay equalizer. The resulting group-delay variation is within 2 ms between about 125 Hz and 16 Hz, which can be assumed to be sufficiently flat to be inaudible. The graphic delay equalizer had the delay sliders set to 1, 3.2 3.2, 3.2, and 3 ms at 1, 2, 4, 8, and 16 kHz, respectively, see the round markers. The number

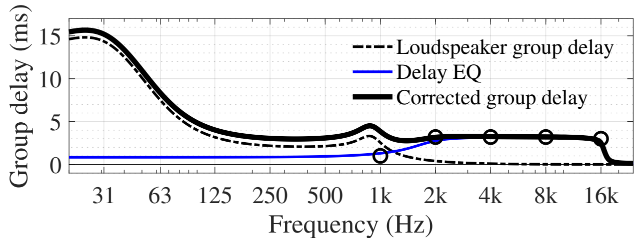


(a)

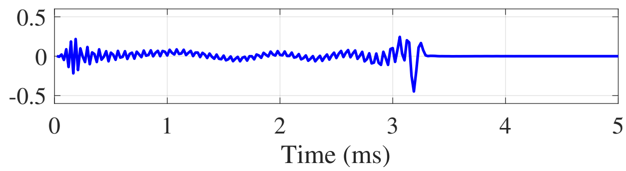


(b)

**Fig. 5**. Loudspeaker group-delay equalization: (a) the group delay of a simulated loudspeaker with the AP delay equalizer and (b) the impulse response of the AP equalizer.

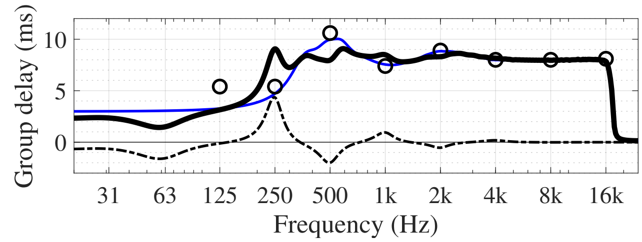


(a)

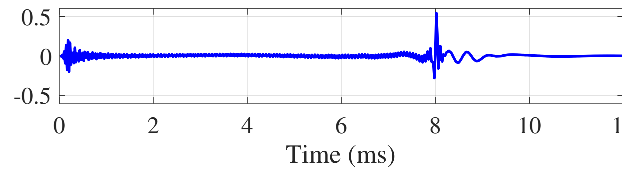


(b)

**Fig. 6**. (a) Group delay equalization of a graphic magnitude equalizer and (b) the resulting impulse response of the AP delay equalizer. See legend in Fig. 5.

of AP sections was 50, there was no additional constant delay, i.e., $d_0 = 0$ ms, while $\beta$ was set to 0.9.

### 4.2. Delay correction for graphic magnitude equalization

Figure 6 shows another use case for the graphic delay equalizer. The dash-dotted line in Fig. 6(a) is the group delay of an octave equalizer, whose gain commands were set to 4, 15, $-8$, 10, and $-10$ dB for octave-spaced center frequencies starting from 125 Hz. As can be seen, the 15-dB peak at 250 Hz creates the largest peak in the group delay, around 4.4 ms. It can cause audible phase distortion [6].

One possible strategy for the group-delay correction is to raise the group delay at high frequencies to the level of the 250-Hz peak. The thin (blue) line shows the response of the delay equalizer, the round markers show the user-defined command delays (including $d_0$), and the thick black line shows the corrected group delay. The command delays were set to 0, 0, 5.2, 2, 3.5, 2.6, 2.6, and 2.7 ms starting from 125 Hz. The number of AP sections was set to 140, which led to a constant delay of $d_0 = 5.4$ ms. The $\beta$ parameter was set to 0.9, with fine-tuning of the first four AP filters, which had $\beta$ of 0.99, 0.62, 0.8, 0.82, respectively. The resulting group-delay deviations are within $\pm 1$ ms between 250 Hz and 16 kHz, which can be assumed to be inaudible.

### 4.3. Comparison with a previous method

Previously, accurate group-delay correction for audio systems has been achieved using a finite impulse response (FIR) filter [7]. Table 1 shows a comparison of the computational load of the proposed AP design and an FIR filter constructed by truncating the impulse responses shown in Figs. 5(b) and 6(b). The FIR filter order is selected so that its magnitude response deviations remain below $\pm 0.5$ dB. The number of operations for an FIR filter of order $N$ is $2N + 1$. A second-order AP filter can be implemented with 5 operations [26], so the number of operations is $2.5N$ for a cascaded AP filter of order $N$. Table 1 shows that the proposed AP-based delay equalizer uses in both cases less operations than an FIR filter. Also, the proposed delay equalizer is more accurate in terms of both the magnitude (completely flat) and group-delay approximation.

## 5. CONCLUSIONS

This paper proposed a graphic delay equalizer allowing users to intuitively change the group-delay characteristics of an audio system. The delay equalizer uses a non-parametric high-order AP filter design method, which automatically estimates the minimum number of AP sections required. Example use cases included the correction of the group delay of a loudspeaker and of a graphic (magnitude) equalizer in order to improve their perceived phase response. The graphic delay equalizer can also be used to create audio effects, for musical instrument modeling, or to create test material for perceptual studies related to phase. Future research could focus on the perception of group-delay equalization, especially with real program material, such as music and speech.

**Table 1**. Comparison of computational loads of FIR and AP filters in terms of operations (OPS) in the two use cases.

| | **Loudspeaker case** | | **Equalizer case** | |
|---|---|---|---|---|
| | FIR | AP (proposed) | FIR | AP (proposed) |
| Order | 156 | 100 | 562 | 280 |
| OPS | 313 | **250** | 1125 | **700** |

## 6. REFERENCES


[1] H. L. F. Helmholtz, *The Sensations of Tone*, Longmans, Green and Co., London, UK, 3rd edition, 1895, orig. German 1877.

[2] R. D. Patterson, "A pulse ribbon model of monaural phase perception," *J. Acoust. Soc. Amer.*, vol. 82, no. 5, pp. 1560–1586, Nov. 1987.

[3] S. P. Lipshitz, M. Pocock, and J. Vanderkooy, "On the audibility of midrange phase distortion in audio systems," *J. Audio Eng. Soc.*, vol. 30, no. 9, pp. 580–595, Sep. 1982.

[4] H. Møller, P. Minnaar, S. K. Olesen, F. Christensen, and J. Plogsties, "On the audibility of all-pass phase in electroacoustical transfer functions," *J. Audio Eng. Soc.*, vol. 55, no. 3, pp. 115–134, Mar. 2007.

[5] M.-V. Laitinen, S. Disch, and V. Pulkki, "Sensitivity of human hearing to changes in phase spectrum," *J. Audio Eng. Soc.*, vol. 61, no. 11, pp. 860–877, Nov. 2013.

[6] J. Liski, A. Mäkivirta, and V. Välimäki, "Audibility of loudspeaker group-delay characteristics," in *Proc. Audio Eng. Soc. 144th Conv.*, Milan, Italy, May 2018.

[7] A. Mäkivirta, J. Liski, and V. Välimäki, "Modeling and delay-equalizing loudspeaker responses," *J. Audio Eng. Soc.*, vol. 66, no. 11, pp. 922–934, Nov. 2018.

[8] D. M. Green, "Temporal acuity as a function of frequency," *J. Acoust. Soc. Amer.*, vol. 54, no. 2, pp. 373–379, 1973.

[9] J. A. Deer, Bloom P. J., and D. Preis, "Perception of phase distortion in all-pass filters," *J. Audio Eng. Soc.*, vol. 33, no. 10, pp. 782–786, Oct. 1985.

[10] M. Karjalainen, E. Piirilä, A. Järvinen, and J. Huopaniemi, "Comparison of loudspeaker equalization methods based on DSP techniques," *J. Audio Eng. Soc.*, vol. 47, no. 1/2, pp. 15–31, Jan./Feb. 1999.

[11] S. Flanagan, B. C. J. Moore, and M. A. Stone, "Discrimination of group delay in clicklike signals presented via headphones and loudspeakers," *J. Audio Eng. Soc.*, vol. 53, no. 7/8, pp. 593–611, Jul./Aug. 2005.

[12] J. Blauert and P. Laws, "Group delay distortions in electroacoustic systems," *J. Acoust. Soc. Amer.*, vol. 63, no. 5, pp. 1478–1483, May 1978.

[13] V. Adam and S. Benz, "Correction of crossover phase distortion using reversed time all-pass IIR filter," in *Proc. Audio Eng. Soc. 122nd Conv.*, Vienna, Austria, May 2007.

[14] S. Bharitkar, C. Kyriakakis, and T. Holman, "Time-alignment of multi-way speakers with group delay equalization—I," in *Proc. Audio Eng. Soc. 124th Conv.*, Amsterdam, The Netherlands, May 2008.

[15] S. Herzog and M. Hilsamer, "Low frequency group delay equalization of vented boxes using digital correction filters," in *Proc. Int. Conf. Digital Audio Effects (DAFX)*, Erlangen, Germany, Sept. 2014.

[16] H.-M. Lehtonen, "Analysis of piano tones using an inharmonic inverse comb filter," in *Proc. Int. Conf. Digital Audio Effects (DAFX)*. Sept. 2008, pp. 333–340, Espoo, Finland.

[17] J. S. Abel, D. P. Berners, S. Costello, and J. O. Smith III, "Spring reverb emulation using dispersive allpass filters in a waveguide structure," in *Proc. Audio Eng. Soc. 121st Conv.*, San Francisco, CA, Oct. 2006.

[18] V. Välimäki, J. Parker, and J. S. Abel, "Parametric spring reverberation effect," *J. Audio Eng. Soc.*, vol. 58, no. 7/8, pp. 547–562, Jul./Aug. 2010.

[19] V. Välimäki, J. S. Abel, and J. O. Smith, "Spectral delay filters," *J. Audio Eng. Soc.*, vol. 57, no. 7/8, pp. 521–531, Jul./Aug. 2009.

[20] E. K. Canfield-Dafilou and J. S. Abel, "Group delay-based allpass filters for abstract sound synthesis and audio effects processing," in *Proc. Int. Conf. Digital Audio Effects (DAFx)*, Aveiro, Portugal, Sept. 2018, pp. 197–204.

[21] J. Rämö, V. Välimäki, and B. Bank, "High-precision parallel graphic equalizer," *IEEE/ACM Trans. Audio Speech Lang. Process.*, vol. 22, no. 12, pp. 1894–1904, Dec. 2014.

[22] V. Välimäki and J. D. Reiss, "All about audio equalization: Solutions and frontiers," *Appl. Sci.*, vol. 6, no. 5, pp. 129, May 2016.

[23] J. S. Abel and J. O. Smith, "Robust design of very high-order allpass dispersion filters," in *Proc. 9th Int. Conf. Digital Audio Effects (DAFx)*, Montreal, Canada, Sept. 2006, pp. 13–18.

[24] J. O. Smith, *Physical Audio Signal Processing*, http://ccrma.stanford.edu/∼jos/pasp/, Online book, 2010, accessed 9 Oct. 2018.

[25] B. C. J. Moore, *An Introduction to the Psychology of Hearing*, Koninklijke Brill NV, Leiden, The Netherlands, 6th edition, 2013.

[26] S. Mitra and K. Hirano, "Digital all-pass networks," *IEEE Trans. Circ. Syst.*, vol. 21, no. 5, pp. 688–700, Sept. 1974.